Robotica: (2021) volume 39, pp. 1997–2007. © The Author(s), 2021. Published by Cambridge University Press.
doi:10.1017/S0263574721000096

Humanoid NAO: A Kinematic Encounter

Chinmaya Sahu†*, Dayal R. Parhi‡, Priyadarshi Biplab Kumar¶, Manoj Kumar Muni§, Animesh Chhotray†† and Krishna Kant Pandey‡‡

†*School of Mechanical Engineering (SMEC), Vellore Institute of Technology Vellore, Vellore 632014, Tamil Nadu, India*
‡*Robotics Laboratory, Mechanical Engineering Department, National Institute of Technology Rourkela, Rourkela 769008, Odisha, India*
E-mail: dayaldoc@yahoo.com
¶*Mechanical Engineering Department, National Institute of Technology Hamirpur, Hamirpur 177005, Himachal Pradesh, India*
E-mail: p.biplabkumar@gmail.com
§*Mechanical Engineering Department, Indira Gandhi Institute of Technology Sarang, Dhenkanal 759146, Odisha, India*
E-mail: manoj1986nitr@gmail.com
††*Department of Mechanical Engineering, Gandhi Institute for Education and Technology, Baniatangi, Bhubaneswar, Khordha 752060, Odisha, India*
E-mail: chhotrayanimesh@gmail.com
‡‡*Department of Mechanical Engineering, G H Raisoni Institute of Engineering and Technology, Pune 412207, Maharashtra, India*
E-mail: kknitrkl@yahoo.in

(Accepted January 8, 2021. First published online: March 2, 2021)

SUMMARY
In the current research, kinematic analysis of a humanoid NAO is attempted. Here, both Denavit–Hartenberg (DH) parameter approach and multibody formulation approach have been analyzed. In the DH parameter approach, the NAO robot is solved by separating it into five individual kinematic chains. In the multibody formulation approach, NAO is divided into 15 segments, and each segment is analyzed. Kinematic analysis holds a significant importance; as from the data obtained in the kinematic analysis, the robots can be designed for real-time path planning and navigation. The current analysis is a novel approach to analyze the NAO based on its kinematic constraints.

KEYWORDS: Constraint equations; DH parameters; Forward kinematics; Humanoid NAO; Multibody formulation.

1. Introduction

Humanoid robots have gained immense popularity among researchers by virtue of their ability to mimic the human behavior unlike other forms of robots. Humanoid robots are primarily aimed at achieving industrial automation in manufacturing and production sectors. The key aim of robotics research has always been to design concepts and models that can assist humans in achieving any set objectives and if required to replace humans in complex and tiresome operations. With a unique ability to mimic the human behavior and capability to work in an environment similar to humans, humanoid robots have always gained first priority compared to all other forms of robots. Human brain is the most complex structure to find in the entire universe, so to prepare a robot that can work

* Corresponding author. E-mail: mechchinu@gmail.com

https://doi.org/10.1017/S0263574721000096 Published online by Cambridge University Press

as a human is, of course, a challenging work. For making a humanoid robot to assist in industrial automation, the navigational parameters need to be designed carefully, which requires a thorough analysis on its kinematics data. Kinematic analysis of several forms of robots has gained attention of researchers in the past. Some of them can be discussed here.

Vukobratovic and Borovac[1] derived a new revolutionary approach for the simplification of robot motion analysis starting from the zero moment point (ZMP) theory. Kim et al.[2] focused on kinematic analysis of a humanoid robot CHP-1 with 12 degrees of freedom (DOF). Sun et al.[3] proposed an inverse displacement analysis of a novel hybrid humanoid robotic arm based on kinematic function realization. Man et al.[4] analyzed the kinematics of a humanoid using screw theory. Korayem and Hoshiar[5] discussed regarding kinematics of cylindrical nanoparticle manipulation with the help of atomic force for a robot on micro scale. Li et al.[6] used Denavit–Hartenberg (DH) formulation approach for dynamic load distribution analysis of a serial–parallel hybrid humanoid arm. Zoday and Pradhan[7] designed a new MTLAB toolbox for inverse kinematic analysis of a robotic gripper capable of operations like grasping. Xu and Li[8] performed kinematic analysis of a micromanipulator based on the physical constraints imposed by both piezoelectric actuators and flexure hinges. Kofinas et al.[9,10] gave a complete analytical solution for the inverse kinematics of the NAO robot. Gonçalves et al.[11] formulated a new kinematic control paradigm for stability analysis of redundant robots. Said et al.[12] formulated a closed form explanation for lower limb kinematics of a humanoid. Hernandez-Santos et al.[13] proposed a new architecture for a biped robot with significant analysis of its gait pattern using kinematic data. Ijspeert[14] reviewed locomotion patterns in robots using central pattern generators. Kumar et al.[15] presented a modular and analytical approach for kinematic analysis of parallel mechanisms. Bagheri et al.[16] designed a new structure to analyze effects of shoulder placement on working of a humanoid. Torabi et al.[17] proposed a control scheme based on adaptive sliding mode control of an exoskeleton robot. Zhou and Tsagarkis[18] designed a kinematic solution toward ankle module of a humanoid. Wang et al.[19] introduced the idea of unscented Kalman filter to control the robotic locomotion. Hera et al.[20] introduced the use of holonomic constraints for a robotic actuator. Yeon and Park[21] gave an idea about foot slip mechanism for sudden turning and change in the direction of locomotion. Hasanpour et al.[22] formulated kinematic solution for Darwin's humanoid robot. Li et al.[23] tried to mimic actual human torso by kinematic simulation of a bioinspired robotic torso. Polverini et al.[24] used kinematics concepts for planning and control of a humanoid robot while it performs heavy object pushing task. Wu and Xie[25] modeled a parallel 3 DOF manipulator kinematics by numerical simulations. Iida et al.[26] gave an idea about accurate leg design for a biped model using reflexive dynamics and elasticity. Rakovic et al.[27] discussed a method of simplification of a complex gait pattern by the use of primitives. Kumar et al.[28–32] used kinematics concepts for complex navigation of humanoid robots in static and dynamic environments. Sanjuan et al.[33] provided kinematic solution for a US-RS-RPS 2-DOF parallel robot both in forward and inverse modes. Korayem et al.[34] studied tracking control and vibration reduction of flexible cable-suspended parallel robots using a robust input shaper. Sayyadi and Babaee[35] designed control of nonholonomic mobile manipulators for cooperative object transportation.

Several researchers have attempted kinematic analysis of mobile robots, but the kinematic analysis of humanoid robots is rarely reported. To be particular, the researchers have not explored the NAO robot fully. Multibody formulation approach is a novel technique that analyzes individual parts of a multibody system, but no case of multibody application on humanoid NAO has been reported. Based on the above shortcomings, the current work is aimed at application of both DH approach and multibody formulation approach for the kinematic analysis of a humanoid NAO. To achieve any form of navigation pattern required for industrial automation, kinematic data serve as a major requirement. Kinematic data help to design actuators and motors required to enable the robot to work in a complex environment and perform the task assigned to it. In the first section of the paper, a humanoid NAO features and specifications are explained in detail and in the subsequent sections; kinematic analysis has been performed using both the above said approaches.

2. Humanoid NAO

Humanoid NAO is a small, programmable humanoid robot designed and developed by ALDEBERAN group of France. Stating with conceptualization in 2004 to replacing Sony's AIBO quadruped robot in 2007, NAO has gone through several modifications and developments. For the

https://doi.org/10.1017/S0263574721000096 Published online by Cambridge University Press

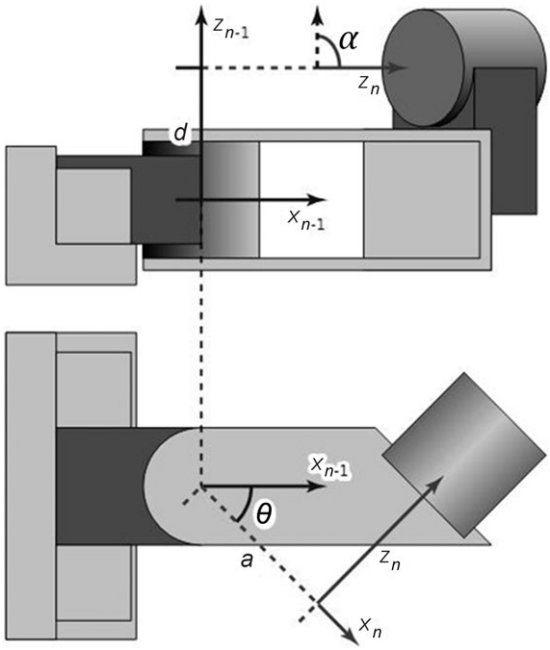


Fig. 1. Representation of DH parameters.

current analysis, version V4 of NAO is used. NAO has 25 DOF. Sensors and actuators are the key elements of the NAO. The sensor network is spread over two cameras, four microphones, two sonars, two IR emitters and receivers, one inertial board, nine tactile sensors and eight pressure sensors. Intel ATOM 1.6 GHz processor is fitted at the head that runs a kernel to support NAOqi software. NAOqi software is Aldebaran's proprietary middleware. NAO has a height of 58 cm and weight of 5 kg.[36]

3. DH Parameters

Denavit–Hartenberg parameters,[37] commonly known as DH parameters, describe a mapping in the form of a function of joint space. In this method, only four parameters are prescribed to completely describe the transformation. These four parameters are named as DH parameters. The parameters are denoted as a, α, d and θ. The parameters can only be described after establishing the reference frame of each joint 'i' with respect to its previous joint as described below.

- The z_i-axis is set along the axis of rotation or the joint axis.
- The x_i-axis is set parallel to the common normal between z_i and z_{i-1} (exterior product).
- The direction of x_i is derived using the right-hand rule from z_{i-1} to z_i.
- The y_i-axis follows from the x_i and z_i axes to form a right-handed coordinate system.

Now, the DH parameters can be described as follows:

a: common normal length
α: angle made at the common normal by z_{i-1}-axis to z_i-axis
d: offset to the common normal along the z_{i-1}-axis
θ: angle made at the z_{i-1}-axis, by x_{i-1}-axis to x_i-axis.

Figure 1 represents a common demonstration of DH parameters.

Three types of transformation matrices are used in the formulation of DH parameter system. Those are basic transformation matrix (T), three rotation matrices about three axes (R_x, R_y, R_z) and a translation matrix (A). In the problem formulation, subscripts can be treated as the starting frames and the superscripts as the destination frames.

4. Kinematic Analysis Using DH Parameters

As in the current investigation, forward kinematics problem is encountered; it would deal with a mapping from the joint coordinate space to the three-dimensional coordinate space. NAO is equipped

https://doi.org/10.1017/S0263574721000096 Published online by Cambridge University Press

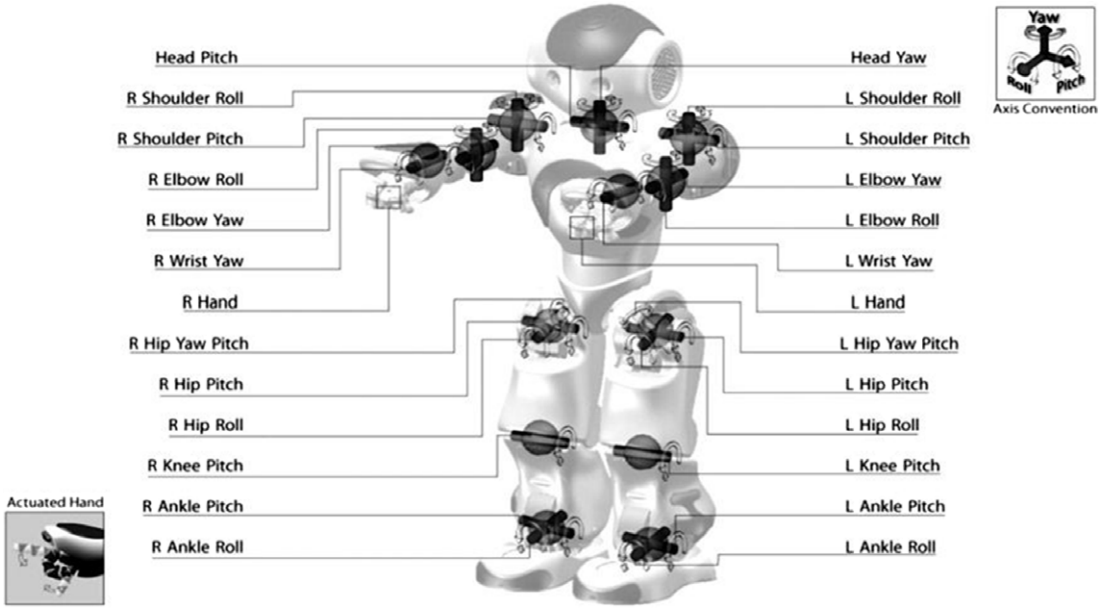


Fig. 2. NAO robot with demonstration of all degrees of freedom and joint rotation.

with 12 bit encoders at each of its joints that operate at a frequency of 100 Hz. During any type of movement of the robot, the current joint values can always be extracted with the help of the above said encoders. As stated earlier, NAO has 25 DOF. If we try to solve the entire NAO as a single kinematic link, it would definitely be a complete chaos. So, to simplify the analysis, NAO can be separated into five individual kinematic chains having a common starting point. As torso is main part of the robot and it is present at the mid-point of the robot, it can be treated as the starting point of each kinematic chain. Hence, NAO can be divided into five chains such as head, two arms and two legs. The first three chains head and two arms are separate from each other. At the same time, it can be argued that both the legs have a common point of contact. However, if the positions of the joints are not disturbed and encoder data are used to only find the joint positions, then two legs can also be assumed to be separate from each other. Now the entire kinematic chain of the NAO robot can be visualized as five independent kinematic chains. If the individual chains can be solved, that would automatically solve the entire kinematic chain. NAO possesses two DOF in head, five DOF on each arm, six DOF on each leg and one DOF in the pelvis, which is common to both the legs at their joint. Figure 2 represents all DOF of NAO.

The joint movements of NAO are as follows:

Head: Head Pitch, Head Yaw
Left Arm: L Shoulder Roll, L Shoulder Pitch, L Elbow Yaw, L Elbow Roll, L Wrist Yaw, L Hand
Right Arm: R Shoulder Roll, R Shoulder Pitch, R Elbow Yaw, R Elbow Roll, R Wrist Yaw, R Hand
Left Leg: L Hip Yaw Pitch, L Hip Pitch, L Hip Roll, L Knee Pitch, L Ankle Pitch, L Ankle Roll
Right Leg: R Hip Yaw Pitch, R Hip Pitch, R Hip Roll, R Knee Pitch, R Ankle Pitch, R Ankle Roll.

It should be noted that L Hip Yaw Pitch and R Hip Yaw Pitch are the common DOF present in the pelvis shared between both the legs.

4.1. Forward kinematics of the head chain

In the entire NAO robot, the head is the simplest kinematic chain. Head possesses two very useful end effectors that are cameras placed at top and bottom. The DH parameters of the head are shown in Table I. The transformation matrix can be given as:

$$T_{Base}^{End} = A_{Base}^{0} T_{0}^{Pos1} T_{Pos1}^{Pos2} R_X(\pi/2) A_{Pos2}^{End} \tag{1}$$

T_0^{Pos1} and T_{Pos1}^{Pos2} represent the DH transformation matrices of the corresponding joints (Head Yaw, Head Pitch). A_{Pos2}^{End} is one of the two translation matrices given in Table I for the two end effectors

https://doi.org/10.1017/S0263574721000096 Published online by Cambridge University Press

Table I. DH parameters of the head chain.

Joint frame	a	α	d	θ
Base		A(0, 0, Neck Offset Z)		
Head Yaw (Pos 1)	0	0	0	θ_1
Head Pitch (Pos 2)	0	$-\pi/2$	0	$\theta_2 - \pi/2$
Rotation		$R_x(\pi/2)R_y(\pi/2)$		
T Camera (Top)		A(T Camera X, 0, T Camera Z)		
B Camera (Bottom)		A(B Camera X, 0, B Camera Z)		
T Camera X = 53.9 mm, T Camera Z = 67.9 mm, B Camera X = 48.8 mm, B Camera Z = 23.8 mm				

Table II. DH parameters of the left arm chain.

Joint frame	a	α	d	θ
Base	A(0, Shoulder Offset Y + Elbow Offset Y, Shoulder Offset Z)			
L Shoulder Pitch (Pos 1)	0	$-\pi/2$	0	θ_1
L Shoulder Roll (Pos 2)	0	$\pi/2$	0	$\theta_2 - \pi/2$
L Elbow Yaw (Pos 3)	0	$-\pi/2$	Upper arm length	θ_3
L Elbow Roll (Pos 4)	0	$\pi/2$	0	θ_4
Rotation		$R_z(\pi/2)$		
End effector		A (Hand Offset X + Lower Arm Length, 0, 0)		

Table III. DH parameters of the right arm chain.

Frame (joint)	a	A	d	θ_1
Base	A(0, -Shoulder Offset Y-Elbow Offset Y, Shoulder Offset Z)			
R Shoulder Pitch (Pos 1)	0	$-\pi/2$	0	θ_2
R Shoulder Roll (Pos 2)	0	$\pi/2$	0	$\theta_2 + \pi/2$
R Elbow Yaw (Pos 3)	0	$-\pi/2$	−Upper arm length	θ_3
R Elbow Roll (Pos 4)	0	$\pi/2$	0	θ_4
Rotation		$R_z(\pi/2)$		
End effector		A(-Hand Offset X-Lower Arm Length, 0, 0)		
Rotation fix		$R_z(-\pi)$		

(top and bottom camera). The point of the end effector in the three-dimensional coordinate space of the torso can be obtained from T_{Base}^{End}.

4.2. Forward kinematics of the left arm chain

The DH parameters of the left arm are shown in Table II, and the final transformation matrix can be given by:

$$T_{Base}^{End} = A_{Base}^{0} T_{0}^{Pos1} T_{Pos1}^{Pos2} T_{Pos2}^{Pos3} T_{Pos3}^{Pos4} R_Z(\pi/2) A_{Pos4}^{End} \tag{2}$$

4.3. Forward kinematics of the right arm chain

The DH parameters for the right arm are shown in Table III, and the final transformation matrix can be given as:

$$T_{Base}^{End} = A_{Base}^{0} T_{0}^{Pos1} T_{Pos1}^{Pos2} T_{Pos2}^{Pos3} T_{Pos3}^{Pos4} R_Z(\pi/2) A_{Pos4}^{End} R_Z(-\pi) \tag{3}$$

https://doi.org/10.1017/S0263574721000096 Published online by Cambridge University Press

Table IV. DH parameters of the left leg chain.

Frame (joint)	***a***	***α***	***d***	***θ***
Base	$A(0$, Hip Offset Y, -Hip Offset $Z)$			
L Hip Yaw Pitch (Pos 1)	0	$-3\pi/4$	0	$\theta_1 - \pi/2$
L Hip Roll (Pos 2)	0	$-\pi/2$	0	$\theta_2 + \pi/4$
L Hip Pitch (Pos 3)	0	$\pi/2$	0	θ_3
L Knee Pitch (Pos 4)	−Thigh length	0	0	θ_4
L Ankle Pitch(Pos 5)	−Thigh length	0	0	θ_5
L Ankle Roll (Pos 6)	0	$-\pi/2$	0	θ_6
Rotation	$\mathrm{R}_z(\pi)\ \mathrm{R}_y(-\pi/2)$			
End effector	$A(0, 0,$ −Foot Height$)$			

Table V. DH parameters of the right leg chain.

Frame (joint)	***a***	***α***	***d***	***θ***
Base	$A(0,$ −Hip Offset $Y,$ −Hip Offset $Z)$			
R Hip Yaw Pitch (Pos 1)	0	$-\pi/4$	0	$\theta_1 - \pi/2$
R Hip Roll (Pos 2)	0	$-\pi/2$	0	$\theta_2 - \pi/4$
R Hip Pitch (Pos 3)	0	$\pi/2$	0	θ_3
R Knee Pitch (Pos 4)	−Thigh length	0	0	θ_4
R Ankle Pitch (Pos 5)	−Thigh length	0	0	θ_5
R Ankle Roll (Pos 6)	0	$-\pi/2$	0	θ_6
Rotation	$Rz(\pi)Ry(-\pi/2)$			
End effector	$A(0, 0,$ −Foot Height$)$			

4.4. Forward kinematics of the left leg chain

The DH parameters of the left leg are shown in Table IV, and the final transformation matrix can be given as:

$$T_{Base}^{End} = A_{Base}^{0} T_{0}^{Pos1} T_{Pos1}^{Pos2} T_{Pos2}^{Pos3} T_{Pos3}^{Pos4} T_{Pos4}^{Pos5} T_{Pos5}^{Pos6} R_Z(\pi) R_Y(-\pi/2) A_{Pos6}^{End} \tag{4}$$

4.5. Forward kinematics of the right leg chain

The DH parameters for the right leg chain are shown in Table V, and the final transformation matrix can be given as:

$$T_{Base}^{End} = A_{Base}^{0} T_{0}^{Pos1} T_{Pos1}^{Pos2} T_{Pos2}^{Pos3} T_{Pos3}^{Pos4} T_{Pos4}^{Pos5} T_{Pos5}^{Pos6} R_Z(\pi) R_Y(-\pi/2) A_{Pos6}^{End} \tag{5}$$

Thus, by solving each individual kinematic chain separately, the whole kinematics of NAO is also solved as discussed in the above sections.

5. Kinematic Analysis Using Multibody Formulation

The kinematic constraints used in the multibody system are aimed at achieving two objectives. First one is to guarantee the rigid body characteristics and second one is to guide the motion of the system. The kinematic constraint equations can be written as:

$$\psi(p, t) = \begin{Bmatrix} \psi_1(p) \\ . \\ \psi_{ns}(p) \\ \psi_{ns+1}(p, t) \\ . \\ \psi_{ns+nr}(p, t) \end{Bmatrix} = 0 \tag{6}$$

https://doi.org/10.1017/S0263574721000096 Published online by Cambridge University Press

where $p = \{p_1, ..., p_n\}$ represent 'n' vector of generalized coordinates and ψ represents 'm' number of kinematic constraints.

As per a general convention

$$m = ns + nr \tag{7}$$

Out of all the kinematic constraints, first 'ns' represents scleronomic constraints and last 'nr' represents rheonomic constraints. It is to note here that scleronomic constraints do not depend on time and rheonomic constraints are explicitly dependent on time.

The above-explained equations are generally not linear in nature. Any iterative scheme can be used to solve these equations. In the current work, Newton Raphson method is used as the iterative scheme to solve the equations. This method is aimed at achieving quadratic convergence near the solution. By linearizing equation and using the first two terms of Taylor's expansion series, the modified equation can be written as:

$$\psi(p, t) \cong \psi(p_j, t) + \psi_p(p_j)(p - p_j) = 0 \tag{8}$$

In the above equation, $\psi_p(p_j)$ is the Jacobian matrix of the constraints evaluated at an approximate solution p_j. The Jacobian matrix has the partial derivative of each kinematic restriction with respect to generalized coordinates. The Jacobian matrix can be written as:

$$\psi_p(p) \equiv \left[\frac{\partial \psi_m}{\partial p_n}\right] = \begin{bmatrix} \frac{\partial \psi_1}{\partial p_1} & \frac{\partial \psi_1}{\partial p_2} & . & \frac{\partial \psi_1}{\partial p_n} \\ \frac{\partial \psi_2}{\partial p_1} & . & . & . \\ . & . & . & . \\ \frac{\partial \psi_m}{\partial p_1} & . & . & \frac{\partial \psi_m}{\partial p_n} \end{bmatrix} \tag{9}$$

As the solution of Eq. (9) does not satisfy the constraint due to approximation, the equation can be rewritten as:

$$\psi_p(p_j)(p - p_j) = \psi(p_j) \tag{10}$$

It should be noted here that vector $\psi(p, t)$ might contain redundant constraints. These redundancies may make the matrix rank deficient. To avoid the above problem, least square formulation may be applied using the following iterative scheme.

$$\psi_p^T(p_j)\psi_p(p_j)(p - p_j) = \psi_p^T\psi(p_j) \tag{11}$$

The above equation is a system of linear equations which is obtained by pre-multiplication of Eq. (10) by the Jacobian matrix transpose. Now the vector of generalized velocities 'p' can be found out by the differentiation of Eq. (6) with respect to time.

$$\psi(p, p, t) \equiv \frac{d\psi(p, t)}{dt} = \psi_p p + \psi_t = 0 \tag{12}$$

In the above equation, ψ_t represents the vector that contains partial derivative of all constraints with respect to time. A ψ_p matrix was already known previously and knowledge about motion can provide the value of ψ_t, so $\dot{p}$ can be determined. Similar to velocity, generalized accelerations can also be found out by differentiation of velocity Eq. (12) with respect to time.

$$\ddot{\psi}(p, \dot{p}, \ddot{p}, t) \equiv \frac{d\dot{\psi}(p, \dot{p}, t)}{dt} = \dot{\psi}_p\dot{p} + \psi_p\ddot{p} + \psi_t = 0 \tag{13}$$

In the above equation, $\dot{\psi}_p$ represents the derivative of the Jacobian matrix with respect to time. $\dot{\psi}_p\dot{p}$ is dependent on velocities calculated in Eq. (13), and $\dot{\psi}_t$ is the derivative of ψ_t with respect to time.

https://doi.org/10.1017/S0263574721000096 Published online by Cambridge University Press

Table VI. Illustrations of rigid body constraints.

Type	Description	*Y*	*X*	L_y	L_x	$<y,x>$
CI	Constant distance between points *i* and *j*	$r_j - r_i$	$r_j - r_i$	*Lij*	*Lij*	0
CII	Constant angle between segments r_{ij} and r_{ik}	$r_j - r_i$	$r_k - r_i$	*Lij*	*Lik*	α
CIII	Constant angle between segments r_{ij} and a unit vector a	$r_j - r_i$	*a*	*Lij*	1	β
CIV	Constant angle between two unit vectors	*a*	*b*	1	1	γ
CV	Unit vector	*a*	*A*	1	1	0

5.1. Kinematic constraint equations

In the current investigation, a mixed coordinate system is used to define the system parameters. In other words, Cartesian coordinate system is mixed with angles to drive the humanoid. In the multibody system, the motion is generated by the actuators located at the joints. As the multibody system is defined with the help of dependent coordinates, a set of kinematic constraint equations need to be formulated to establish a relation among these variables. Here, two types of constraint equations are used such as rigid body constraints and driver constraints. The rigid body constraints are aimed at ensuring a rigid body configuration and the driver constraints are aimed at smoothly driving the motion.[38]

5.2. Rigid body constraints

A rigid body can be characterized by a set of specific points and unit vectors. Several combinations of these points and unit vectors can define a rigid body. In the humanoid configuration, two local unit vectors are associated with each segment to determine the absolute orientation.

Total number of constraints required to define completely a segment is directly dependent upon the number of points and vectors associated with that segment. Even if all the kinematic constraints bear a different physical meaning, all of them can be mathematically expressed by scalar product of two unit vectors '*x*' and '*y*'. The mathematical relation can be written as follows:

$$\psi(p,t) = y^T x - L_x L_y \cos\left(\langle y, x\rangle\,(t)\right) = 0 \tag{14}$$

where L_x and L_y represent length of vectors x and y and $\langle y, x\rangle\,(t)$ is the angle between both the vectors at time t. The rigid body constraints that are used in the current investigation are listed in Table VI.

As stated earlier, the linear dependency also needs to be introduced by another two constraints named as CVI and CVII. CVI would represent a vector '*d*' as a linear combination of a vectorial basis. The base can be defined using a vector '*e*' and two points of body segment '*ij*' and '*ik*'.

$$CVI\,\psi(p,t) = d - a(r_j - r_i) - b(r_k - r_i) - ce = 0 \tag{15}$$

In the above equation, *a*, *b* and *c* represent coefficients of linear combination.

Similarly, CVII constraint would help to find out local position of an extra point (point *q*) as a linear combination of previous vectorial basis.

$$CVI\,\psi(p,t) = (r_q - r_i) - f(r_j - r_i) - g(r_k - r_i) - he = 0 \tag{16}$$

where *d*, *e* and *f* represent coordinates of vector $r_q - r_i$.

As an example, the pelvis segment of the humanoid NAO can be formulated using the kinematic constraint equations as shown in Fig. 3.

Pelvis segment of the NAO humanoid is defined using three points (P_1, P_2, P_3) and two vectors x_p and y_p. As a result, total 15 variables are associated with this segment, so 9 constraint equations can be defined for this segment. Out of the nine constraint equations, two guarantee constant distance between joints P_1 and P_2 (L_{12}) and between P_1 and P_3 (L_{13}). These two constraints are of CI type as demonstrated in Table VI. Another constraint ensures constant angle between vectors r_{P_1}-r_{P_2} and r_{P_3}-r_{P_1}. This constraint is of CII type. Two more constraints guarantee constant angle between vectors x_p and segment P_1P_3 (γ). These two are of CIII type. The last constraint guarantees x_p as a unit vector.

https://doi.org/10.1017/S0263574721000096 Published online by Cambridge University Press

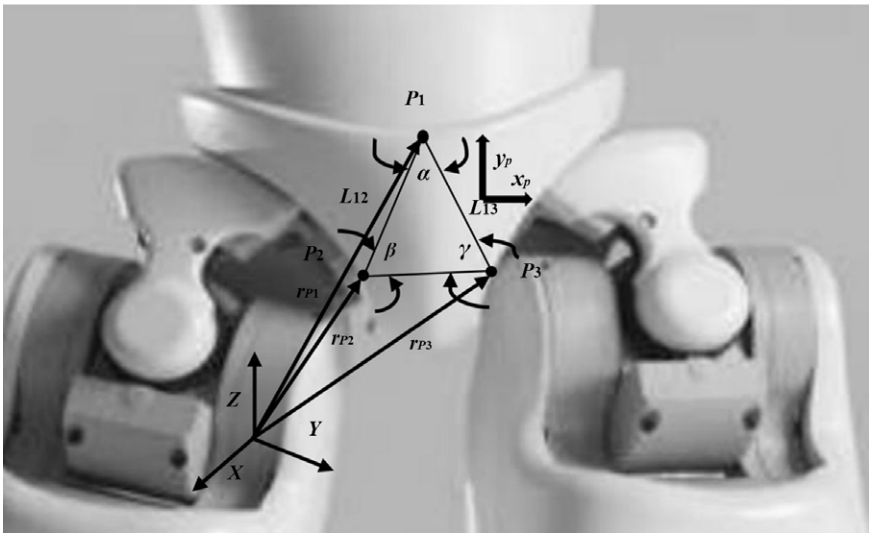


Fig. 3. Kinematic constraints of pelvis segment.

This is of CV type. Now all the above-mentioned constraints can be mathematically expressed using the following algebraic equations:

$$\text{CI}\left(r_{p2}-r_{p1}\right)^{T}\left(r_{p2}-r_{p1}\right)-L_{12}^{2}=0 \tag{17}$$

$$\text{CI}\left(r_{p3}-r_{p1}\right)^{T}\left(r_{p3}-r_{p1}\right)-L_{13}^{2}=0 \tag{18}$$

$$\text{CII}\left(r_{p2}-r_{p1}\right)^{T}\left(r_{p3}-r_{p1}\right)-L_{12}L_{13}\cos\alpha=0 \tag{19}$$

$$\text{CIII}\left(r_{p2}-r_{p1}\right)^{T}x_{p}-L_{12}\cos\beta=0 \tag{20}$$

$$\text{CIII}\left(r_{p3}-r_{p1}\right)^{T}x_{p}-L_{13}\cos\gamma=0 \tag{21}$$

$$\text{CV}x_{p}^{T}x_{p}-1^{2}=0 \tag{22}$$

The above-mentioned six constraints are determined using Table VI. Three more constraints are required to establish the linear dependency between the generalized coordinates. Vector y_p can be formulated as a combination of three joint points $P1$, $P2$, $P3$ and a vector x_p. The mathematical expression can be written as follows:

$$y_{p}-a(r_{P2}-r_{P1})-b(r_{P3}-r_{P1})-cx_{p}=0 \tag{23}$$

5.3. Driver constraints

As discussed before, driver constraints are specified to easily drive the motion of the humanoid. A rigid body orientation can be imposed by three basis rotations about the three orthogonal axes that can be represented as follows:

$$R_{i}=R_{\gamma}R_{\beta}R_{\alpha} \tag{24}$$

where R_i is the rotation matrix and

$$R_{\alpha}=\begin{bmatrix}1&0&0\\0&\cos\alpha&-\sin\alpha\\0&\sin\alpha&\cos\alpha\end{bmatrix},\ R_{\beta}=\begin{bmatrix}\cos\beta&0&\sin\beta\\0&1&0\\-\sin\beta&0&\cos\beta\end{bmatrix},\ R_{\gamma}=\begin{bmatrix}\cos\gamma&-\sin\gamma&0\\\sin\gamma&\cos\gamma&0\\0&0&1\end{bmatrix} \tag{25}$$

As a result, a vector 'd' belonging to one rigid segment can be expressed in terms of a vector 'e' of global reference frame with the help of transformation as:

https://doi.org/10.1017/S0263574721000096 Published online by Cambridge University Press

$$d = R_i e \tag{26}$$

$$d - R_\gamma R_\beta R_\alpha e = 0 \tag{27}$$

To calculate the three absolute angles used in the rotation matrices, two unit vectors of local reference frame need to be expressed in terms of unit vectors of global reference frame. For the pelvis segment, αp, βp and γp can be found out by solving the following equations:

$$x_p - R_{\gamma p} R_{\beta p} R_{\alpha p} x_x = 0 \tag{28}$$

$$y_p - R_{\gamma p} R_{\beta p} R_{\alpha p} y_z = 0 \tag{29}$$

In the above two equations, x_p and y_p represent the unit vectors of pelvis segment, and x_x and y_z are unit vectors of global reference frame. Similarly, all the other segments of the humanoid NAO can be solved for the driver constraints. The multibody system is represented by the use of specific joints and absolute angles α, β and γ of each segment with respect to the global reference frame. Now to express the motion of the multibody system, the following driver constraints can be used:

$$\phi_i - \phi_i(t) = 0 \tag{30}$$

$$r_{p1} - r_{p1}(t) = 0 \tag{31}$$

where ϕ_i is the absolute angular coordinates and $\phi_i(t)$ represents the corresponding analytical expression. r_{p1} is the absolute position of point P_1 and $r_{p1}(t)$ is the corresponding analytical expression.

Here, the analysis of both rigid body constraints and driver constraints solves the purpose of whole body kinematic analysis of NAO humanoid.

6. Conclusion

With the increasing demand toward achieving industrial automation, humanoid robots have become a non-separable entity in production and manufacturing industries. A humanoid needs to think, walk, work and perceive like a human to attain the above objectives. In an automation industry, the gait pattern and navigational analysis would serve as the two most important aspects of design. To do the same, kinematic analysis of the humanoid robots is necessary. The current paper analyzes the kinematic parameters of a NAO humanoid robot, but the same analysis can also be expanded to any kind of humanoid and toward navigational analysis also. Here, the kinematic analysis deals with a NAO humanoid only. However, a more generalized form of analysis can be proposed applicable to any robot irrespective of its form. The analysis can also be extended for the dynamic analysis of the humanoid robots required for designing a dynamic navigational controller. To conclude the research, the authors expect the analysis to be very much helpful to all the researchers and personnel working in industry, and it will definitely add a new dimension to the humanoid research.

References

1. M. Vukobratović and B. Borovac, "Zero-moment point-thirty five years of its life," *Int. J. humanoid Rob.* **1**(01), 157–173 (2004).
2. D. U. Kim, S.W. Hwang, H. J. Kang and D. S. Hong, "Kinematic analysis of a humanoid robot CHP-1 and selection of motors in consideration of cooperative motion," *J. Central South Univ.* **19**(11), 3094–3099 (2012).
3. P. Sun, Y. Li, Z. Wang, K. Chen, B. Chen, X. Zeng, J. Zhao and Y. Yue, "Inverse displacement analysis of a novel hybrid humanoid robotic arm," *Mech. Mach. Theory* **147**(147), 103743 (2020).
4. C. H. Man, F. Xun, C. R. Li and Z. H. Zhao, "Kinematics analysis based on screw theory of a humanoid robot," *J. China Univ. Mining Technol.* **17**(1), 49– 52 (2007).
5. M. H. Korayem and A. K. Hoshiar, "3D kinematics of cylindrical nanoparticle manipulation by an atomic force microscope based nanorobot," *Scientia Iranica* **21**(6), 1907–1919 (2014).
6. Y. Li, L. Wang, B. Chen, Z. Wang, P. Sun, H. Zheng, T. Xu and S. Qin, "Optimization of dynamic load distribution of a serial-parallel hybrid humanoid arm," *Mech. Mach. Theory* **149**(149), 103792 (2020).
7. S. Zodey and S. K. Pradhan, "Matlab toolbox for kinematic analysis and simulation of dexterous robotic grippers," *Procedia Eng.* **97**, 1886–1895 (2014).
8. Q. Xu and Y. Li, "Kinematic analysis and optimization of a new compliant parallel micromanipulator," *Int. J. Adv. Rob. Syst.* **3**(4), 47 (2006).

https://doi.org/10.1017/S0263574721000096 Published online by Cambridge University Press

9. N. Kofinas, E. Orfanoudakis and M. G. Lagoudakis, "Complete Analytical Inverse Kinematics for NAO," *13th International Conference on Autonomous Robot Systems (Robotica)* (2013) pp. 1–6.
10. N. Kofinas, E. Orfanoudakis and M. G. Lagoudakis, "Complete analytical forward and inverse kinematics for the NAO humanoid robot," *J. Intell. Rob. Syst.* **77**(2), 251–264 (2015).
11. V. M. Gonçalves, B. V. Adorno, A. Crosnier and P. Fraisse, "Stable-by-design kinematic control based on optimization," *IEEE Trans. Rob.* **36**(3), 644– 656 (2020).
12. A. Said, E. Rodriguez-Leal, R. Soto, J. L. Gordillo and L. Garrido, "Decoupled closed- form solution for humanoid lower limb kinematics," *Math. Probl. Eng.* (2015). doi: 10.1155/2015/437979.
13. C. Hernández-Santos, E. Rodriguez-Leal, R. Soto and J. L. Gordillo, "Kinematics and dynamics of a new 16 DOF humanoid biped robot with active toe joint," *Int. J. Adv. Rob. Syst.* **9**(5), 190 (2012).
14. A. J. Ijspeert, "Central pattern generators for locomotion control in animals and robots: A review," *Neural Networks* **21**(4), 642–653 (2008).
15. S. Kumar, K. A. V. Szadkowski, A. Mueller and F. Kirchner, "An analytical and modular software workbench for solving kinematics and dynamics of series-parallel hybrid robots," *J. Mech. Rob.* **12**(2), (2020). doi: 10.1115/1.4045941.
16. M. Bagheri, A. Ajoudani, J. Lee, D. G. Caldwell and N. G. Tsagarakis, "Kinematic Analysis and Design Considerations for Optimal Base Frame Arrangement of Humanoid Shoulders," *2015 IEEE International Conference on Robotics and Automation (ICRA)* (IEEE, 2015) pp. 2710–2715.
17. M. Torabi, M. Sharifi and G. Vossoughi, "Robust adaptive sliding mode admittance control of exoskeleton rehabilitation robots," *Scientia Iranica* **25**(5), 2628–2642 (2018).
18. C. Zhou and N. Tsagarakis, "On the comprehensive kinematics analysis of a humanoid parallel ankle mechanism," *J. Mech. Rob.* **10**(5), 051015 (2018).
19. L. Wang, Z. Liu, C. P. Chen, Y. Zhang, S. Lee and X. Chen, "A UKF-based predictable SVR learning controller for biped walking," *IEEE Trans. Syst. Man Cybern. Syst.* **43**(6), 1440–1450 (2013).
20. P. X. M. La Hera, A. S. Shiriaev, L. B. Freidovich, U. Mettin and S. V. Gusev, "Stable walking gaits for a three-link planar biped robot with one actuator," *IEEE Trans. Rob.* **29**(3), 589–601 (2013).
21. J. S. Yeon and J. H. Park, "A fast turning method for biped robots with foot slip during single-support phase," *IEEE/ASME Trans. Mech.* **19**(6), 1847–1858 (2014).
22. A. Hasanpour, P. Daemy, M. Aghazamani, K. Alipour and M. Jafari, "Kinematic Analysis of Darwin's Humanoid Robot," *2016 4th International Conference on Control, Instrumentation, and Automation (ICCIA)* (IEEE, 2016) pp. 356–361.
23. T. Li, P. Yao, M. Luo, Z. Tan, M. Wang and Z. Guo, "Design and kinematics analysis of a novel six-degree-of-freedom serial humanoid torso," *Int. J. Adv. Rob. Syst.* **15**(1), 1729881417748126 (2017).
24. M. P. Polverini, A. Laurenzi, E. M. Hoffman, F. Ruscelli and N. G. Tsagarakis, "Multi-contact heavy object pushing with a centaur-type humanoid robot: Planning and control for a real demonstrator," *IEEE Rob. Autom. Lett.* **5**(2), 859–866 (2020).
25. X. Wu and Z. Xie, "Forward kinematics analysis of a novel 3-DOF parallel manipulator," *Scientia Iranica Trans. B Mech. Eng.* **26**(1), 346–357 (2019).
26. F. Iida, Y. Minekawa, J. Rummel and A. Seyfarth, "Toward a human-like biped robot with compliant legs," *Robot. Auton. Syst.* **57**(2), 139–144 (2009).
27. M. Rakoviæ, B. Borovac, M. Nikoliæ and S. Savić, "Realization of biped walking in unstructured environment using motion primitives," *IEEE Trans. Rob.* **30**(6), 1318–1332 (2014).
28. P. B. Kumar, M. K. Muni and D. R. Parhi, "Navigational analysis of multiple humanoids using a hybrid regression-fuzzy logic control approach in complex terrains," *Appl. Soft Comput.* **89**(89), 106088 (2020).
29. P. B. Kumar, C. Sahu and D. R. Parhi, "Intelligent navigation of a self-fabricated biped robot using a regression controller," *Scientia Iranica* **27**(1), 262–272 (2020).
30. A. K. Rath, H. C. Das, D. R. Parhi and P. B. Kumar, "Application of artificial neural network for control and navigation of humanoid robot," *J. Mech. Eng. Sci.* **12**(2), 3529–3538 (2018).
31. P. B. Kumar and D. R. Parhi, "Intelligent hybridization of regression technique with genetic algorithm for navigation of humanoids in complex environments," *Robotica* **38**(4), 565–581 (2020).
32. P. B. Kumar, C. Sahu, D. R. Parhi, K. K. Pandey and A. Chhotray, "Static and dynamic path planning of humanoids using an advanced regression controller," *Scientia Iranica* **26**(1), 375–393 (2019).
33. J. Sanjuan, D. Serje and J. Pacheco, "Closed form solution for direct and inverse kinematics of a US-RS-RPS 2-DOF parallel robot," *Scientia Iranica Trans. B Mech. Eng.* **25**(4), 2144–2154 (2018).
34. M. H. Korayem, M. Yousefzadeh and S. Manteghi, "Tracking control and vibration reduction of flexible cable-suspended parallel robots using a robust input shaper," *Scientia Iranica Trans. B Mech. Eng.* **25**(1), 230–252 (2018).
35. H. Sayyaadi and M. Babaee, "Control of nonholonomic mobile manipulators for cooperative object transportation", *Scientia Iranica Trans. B Mech. Eng.* **21**(2), 347 (2014).
36. A. Robotics "Nao software 1.14.5 documentation," http://www. Aldebaran- robotics.com.
37. J. Denavit, "A kinematic notation for lower-pair mechanisms based on matrices," *ASME J. Appl. Mech.*, 215–221 (1955).
38. R. Pàmies-Vilà, J. M. Font-Llagunes, J. Cuadrado and F. J. Alonso, "Analysis of different uncertainties in the inverse dynamic analysis of human gait," *Mech. Mach. Theory* **58**(58), 153–164 (2012).

https://doi.org/10.1017/S0263574721000096 Published online by Cambridge University Press